Original Article

DOI: 10.5582/bst.2025.01302

The dual role of TRPA1 in dextran sulfate sodium (DSS)-induced murine colitis: Suppression alleviates acute inflammation but exacerbates subacute disease

Fangzhou Dou[1,§], Jing Li[1,§], Daoran Lu[1], Yueyi Sun[1], Shasha Hu[2,*], Jianjun Gao[1,*]

[1] Department of Pharmacology, School of Pharmacy, Qingdao Medical College, Qingdao University, Qingdao, Shandong, China;
[2] Department of Pathology, The Affiliated Hospital of Qingdao University, Qingdao, Shandong, China.

SUMMARY: Ulcerative colitis (UC) is a chronic inflammatory bowel disease with limited treatment options. Transient receptor potential ankyrin 1 (TRPA1) has been implicated in inflammation and pain, but its role in UC remains a subject of debate. The current study investigated the effects of TRPA1 inhibition in both acute and subacute murine models of dextran sulfate sodium (DSS)-induced colitis. Genetic knockout of *Trpa1* or pharmacological inhibition with A967079 significantly ameliorated inflammation in the acute model, reducing the disease activity index (DAI), colon shortening, histopathological damage, and TNF-α secretion from macrophages. In contrast, TRPA1 suppression exacerbated subacute colitis and worsened weight loss, DAI, colon shortening, and histopathology. Mechanistically, *Trpa1* deletion promoted $CD4^+$ T cell polarization toward the Th1 subtype in subacute colitis, increasing IFN-γ levels. These findings reveal a dual role for TRPA1 in colonic inflammation: it mediates pro-inflammatory effects primarily *via* innate immune cells in the acute phase but has anti-inflammatory effects by modulating adaptive immunity in the subacute phase. These findings provide new insights into the context-dependent roles of TRPA1 and suggest that TRPA1 may represent a context-specific and stage-dependent therapeutic target in UC.

Keywords: TRPA1, inflammatory bowel disease, ulcerative colitis, animal model

1. Introduction

Ulcerative colitis (UC) is a chronic, idiopathic inflammatory bowel disease characterized by continuous inflammation of the colonic mucosa and submucosa, clinically presenting with recurrent diarrhea, bloody and mucopurulent stools, and abdominal pain (*1*). Global epidemiological data indicate a rising incidence and prevalence, particularly in industrialized nations, imposing a substantial disease burden and significantly diminishing patients' quality of life (*2-5*).

Current pharmacotherapeutic strategies primarily encompass 5-aminosalicylic acid (5-ASA) compounds (for inducing and maintaining remission in mild-to-moderate disease), corticosteroids (for inducing remission in moderate-to-severe disease), immunosuppressants (*e.g.*, azathioprine for maintenance therapy), and biological agents (*e.g.*, anti-TNF-α monoclonal antibodies) (*2,6-8*). However, existing therapies have notable limitations, as a substantial proportion of patients exhibit primary non-response or experience a loss of therapeutic efficacy over time (*9*). Consequently, there is a pressing clinical need to develop innovative therapeutics with novel mechanisms of action, sustained efficacy, and improved safety profiles in order to achieve deep and durable remission in a greater proportion of patients and to improve long-term clinical outcomes.

Transient receptor potential ankyrin 1 (TRPA1) is a member of the TRP ion channel family and is predominantly expressed in sensory neurons, epithelial cells, and immune cells (*10,11*). Functioning as a polymodal nocisensor, it is activated by environmental stimuli (*e.g.*, cold and mechanical force), endogenous inflammatory mediators (*e.g.*, reactive oxygen species and prostaglandins), and exogenous compounds (*e.g.*, mustard oil), mediating Ca^{2+} influx (*12,13*). Under pathological conditions, TRPA1 activation directly contributes to nociceptive signaling and the initiation of neurogenic inflammation (*14*). By promoting the release of neuropeptides such as substance P and calcitonin gene-related peptide (CGRP), it amplifies local vasodilation, plasma extravasation, and immune cell infiltration, playing a pivotal role in chronic pain conditions (*e.g.*, neuropathic pain and visceral pain) and inflammatory diseases (*e.g.*, asthma and dermatitis) (*15,16*). Its potential as an anti-inflammatory and analgesic target has been

substantiated by preclinical studies, demonstrating that targeted inhibition significantly alleviates inflammatory responses and pain hypersensitivity (*17*). However, the role of TRPA1 inhibition in UC—whether it has an anti-inflammatory or pro-inflammatory effect—remains a subject of debate (*18,19*). The role of TRPA1 activation in intestinal immune cells in modulating innate and adaptive immune responses needs to be further elucidated.

The current study used both acute and subacute murine colitis models to investigate the role of TRPA1 across distinct inflammatory milieus. The acute model reflects an inflammatory environment predominantly driven by innate immune responses, whereas the subacute model additionally engages adaptive immunity. Results revealed a dual role for TRPA1 in colonic inflammation: inhibition of TRPA1 had anti-inflammatory effects in the acute inflammatory milieu, while TRPA1 inhibition promoted pro-inflammatory responses in the subacute inflammatory milieu. This dichotomous behavior of TRPA1 may be attributable to its distinct functions in macrophages and $CD4^+$ T cells. Collectively, these findings provide new insights into the context-dependent roles of TRPA1 and suggest that TRPA1 may represent a context-specific and stage-dependent therapeutic target in UC.

2. Materials and Methods

2.1. Reagents and animals

Reagents and materials were sourced as follows: dextran sulfate sodium (DSS) (MW 40,000) and 5-aminosalicylic acid (5-ASA) were purchased from Shanghai Aladdin Biochemical Technology Co., Ltd. (Shanghai, China). A967079 and lipopolysaccharide (LPS) were obtained from Sigma-Aldrich (St. Louis, MO, USA). A hematoxylin and eosin (H&E) staining kit, Alcian blue staining kit, and periodic acid-Schiff (PAS) staining kit were acquired from Beijing Solarbio Science & Technology Co., Ltd. (Beijing, China). A Cell Counting Kit-8 (CCK-8) assay kit was supplied by Shanghai Topscience Co., Ltd. (Shanghai, China). Ficoll-Paque PREMIUM 1.084 was obtained from Cytiva (Marlborough, MA, USA). Fixable Viability Stain 780, Mouse BD Fc Block, BD™ CompBeads Anti-Rat Ig, κ/Negative Control Compensation Particles Set, and BB700 Rat Anti-Mouse CD4 (RM4-5) were sourced from BD Biosciences (Franklin Lakes, NJ, USA). The following antibodies were from BioLegend (San Diego, CA, USA): FITC anti-mouse CD3, APC anti-mouse CD25, Brilliant Violet 421™ anti-mouse IL-17A, PE anti-mouse FOXP3, Brilliant Violet 650™ anti-mouse IFN-γ, and PE/Cyanine7 anti-mouse IL-4. A Mouse IL-17A ELISA Kit and Mouse TNF-α ELISA Kit were purchased from Wuhan ABclonal Biotechnology Co., Ltd. (Wuhan, China). A Mouse IFN-γ ELISA Kit was acquired from Shanghai Absin Bioscience Inc. (Shanghai, China). An Intracellular Fixation/Permeabilization Buffer Kit was obtained from Wuhan Elabscience Biotechnology Co., Ltd. (Wuhan, China).

Wild-type (WT) C57BL/6N mice were purchased from Beijing Vital River Laboratory Animal Technology Co., Ltd. (Beijing, China). *Trpa1*$^{+/-}$ C57BL/6N mice were purchased from Cyagen Biosciences Co., Ltd. (Jiangsu, China). The *Trpa1*$^{-/-}$ mice and WT mice that were used to compare the effects of gene knockout were bred from the aforementioned heterozygous mice. All experimental animals were housed in a specific pathogen-free environment, and the mice had free access to water and food. All experimental procedures strictly adhered to international guidelines for the care and use of laboratory animals, and the protocols were approved by the Ethics Committee of the Medical College of Qingdao University (20230324C5719220250105064).

2.2. Protocol for the effect that suppressing TRPA1 had on acute colitis in mice

Impact of Trpa1 knockout on acute colitis in mice. Female C57BL/6N WT and *Trpa1*$^{-/-}$ mice, age 8-10 weeks, were selected. After a one-week acclimatization period, WT mice were randomly divided into: a normal control (NC) group and a DSS treatment group (WT+DSS). Concurrently, *Trpa1*$^{-/-}$ mice were assigned to a DSS treatment group (*Trpa1*$^{-/-}$+DSS). Each group consisted of 5-8 mice. From days 1 to 7, the WT+DSS and *Trpa1*$^{-/-}$+DSS groups had access to a 2.5% DSS solution *ad libitum*, while the NC group received sterile drinking water. Throughout the experiment, body weight, general condition, fecal consistency, and intestinal bleeding were monitored daily. The disease activity index (DAI) was calculated according to the criteria outlined in Table S1 (*https://www.biosciencetrends.com/action/getSupplementalData.php?ID=282*). On day 7, mice were euthanized. The colon and spleen were collected, and colon length and spleen weight were measured and recorded. Colon tissue sections were prepared for histological analysis, including hematoxylin and eosin (HE) staining, Alcian blue staining, and periodic acid-Schiff (PAS) staining. Remaining tissue samples were stored at -80°C.

Impact of a TRPA1 inhibitor on acute colitis in mice. Female C57BL/6N WT mice (8-10 weeks old) were acclimatized for 1-2 weeks and subsequently randomized into four experimental groups (n = 5-7 per group): an NC group, a colitis model (DSS+vehicle) group, an A967079 intervention (DSS+A967079) group, and a positive control (DSS+5-ASA) group. During the modeling phase (days 1-7), all groups except the NC group had access to a 2.5% DSS solution *ad libitum*, while the NC group received sterile drinking water. Pharmacological interventions commenced on the first day of modeling: the DSS+A967079 group received 10 mg/kg A967079 *via* oral gavage twice

daily (BID), the DSS+5-ASA group received 200 mg/kg 5-ASA *via* gavage BID, and the DSS+vehicle group received the drug formulation vehicle *via* gavage BID. Daily monitoring included body weight measurement, assessment of general condition, fecal consistency, and intestinal bleeding, with the DAI calculated according to the criteria in Table S1 (*https://www.biosciencetrends.com/action/getSupplementalData.php?ID=282*). On day 7, mice were euthanized for tissue collection; colon length was measured, spleen weight was recorded, and colon tissues were processed for HE histological analysis. Residual tissues were cryopreserved at -80°C.

2.3. Protocol for the effect that suppressing TRPA1 had on subacute colitis in mice

Impact of Trpa1 knockout on subacute colitis in mice. Female C57BL/6N WT and *Trpa1*$^{-/-}$ mice, age 8-10 weeks, were selected. After a one-week acclimatization period, WT mice were randomly divided into: an NC group (n = 8) and a DSS treatment group (WT+DSS, n = 8). *Trpa1*$^{-/-}$ mice were assigned to the DSS treatment group (*Trpa1*$^{-/-}$+DSS, n = 8). From day 0 to 30, both the WT+DSS group and the *Trpa1*$^{-/-}$+DSS group mice had access to a 1.0% DSS solution *ad libitum*. From day 31 to 45, these groups had access to a 1.5% DSS solution *ad libitum*. Mice in the NC group had access to water *ad libitum* from Day 1-45. During the experimental period, body weight was recorded every 3 days. The mouse's status, fecal consistency, and intestinal bleeding were observed, and the DAI was calculated according to the criteria detailed in Table S1 (*https://www.biosciencetrends.com/action/getSupplementalData.php?ID=282*). On day 45, mice were euthanized, and the colon and spleen were harvested. Colon length and spleen weight were measured. Colon tissues were subjected to histological analysis including H&E staining, Alcian blue staining, and PAS staining. The remaining tissues were stored at -80°C.

Impact of a TRPA1 inhibitor on subacute colitis in mice. Female C57BL/6N WT mice (age 8-10 weeks) were acclimatized for one week. Three mice were then randomly assigned to the NC group and given access to water *ad libitum*. The remaining 18 mice had access to a 1% DSS solution *ad libitum* for 30 days. On day 31, the mice treated with DSS were randomly divided into three groups (n = 6/group): a model group (DSS+vehicle), an A967079 intervention group (DSS+A967079), and a positive control group (DSS+5-ASA). From day 31 onward, the DSS concentration was increased to 1.5% for all groups except the NC group, which continued receiving water. Concurrent with the increase to 1.5% DSS, drug intervention was initiated. Mice in the DSS+A967079 group received A967079 (10 mg/kg) *via* oral gavage BID. Mice in the DSS+5-ASA group received 5-ASA (200 mg/kg) *via* oral gavage BID. Mice in the DSS+vehicle group received the corresponding vehicle *via* oral gavage BID. This treatment regimen was maintained for 10-15 days. Throughout the modeling period, body weight and symptoms (diarrhea and fecal blood) were recorded every 3 days. At the experimental endpoint, the DAI was calculated. Mice were then euthanized, tissues were harvested, and colon length was measured.

2.4. H&E, Alcian blue, and PAS staining

Fresh colon tissues were fixed in 4% paraformaldehyde for 24 h, followed by dehydration, embedding in paraffin, and sectioning using standard histological protocols. Sections were dried overnight at 37°C. After deparaffinization in xylene and rehydration through a graded ethanol series, staining procedures were performed. For H&E staining, sections were stained with hematoxylin for 5 min, differentiated in 0.5% acid alcohol for 2-5 s, rinsed in running water for 20 min for blue development, counterstained with eosin for 1 min, and rinsed with water. For Alcian blue staining, sections were treated with an acidification solution for 3 min, incubated with Alcian blue stain in a humid chamber for 30 min at room temperature (RT), rinsed with water (3×1 min), counterstained with Nuclear Fast Red (5 min), and rinsed (1 min). For PAS staining, sections were oxidized with periodic acid (5-8 min, RT), rinsed with water (2-3 min), washed with distilled water (2×3 min), incubated in Schiff's reagent (15 min, dark), rinsed with water (10 min), stained with hematoxylin (1-2 min), differentiated in an acid solution (2-5 s), and rinsed for blue development (10-15 min). All sections were dehydrated in graded ethanol, cleared in xylene, and mounted with neutral balsam. After fume hood drying, whole-slide scanning was performed. Histopathological scoring of H&E-stained sections followed the criteria in Table S2 (*https://www.biosciencetrends.com/action/getSupplementalData.php?ID=282*).

2.5. CCK-8 assay

Cells were cultured in T25 flasks until reaching ~90% confluency and then trypsinized and resuspended in fresh medium to achieve an appropriate density. The cell suspension (100 µL/well) was seeded onto a 96-well plate. After incubation at 37°C overnight in a 5% CO_2 humidified incubator to allow cell attachment, test compounds were added and incubated for 24 h. Following removal of compound-containing medium, 150 µL of CCK-8 working solution (prepared by mixing 1 mL CCK-8 stock with 9 mL PBS) was added to each well. The plate was returned to the incubator for 1 h, after which absorbance at 450 nm was measured using a microplate reader.

2.6. RAW264.7 cell culture and tumor necrosis factor-α (TNF-α) detection

Mouse RAW 264.7 cells were cultured to 80-90% confluency, after which the spent medium was aspirated and monolayers were gently washed with 2 mL of pre-warmed PBS. Following PBS removal, adherent cells were detached by gentle pipetting with fresh medium to generate a single-cell suspension. The suspension was adjusted to a density of 2.5×10^5 cells/mL with additional medium, and 2-mL aliquots were seeded per well on 6-well plates. Plates were gently agitated for uniform distribution and incubated overnight in a humidified 37°C/5% CO_2 incubator. The following day, after confirming cell attachment, the medium was aspirated and replaced with 2 mL of compound-containing medium at specified concentrations per experimental design, followed by incubation for 2 h. Subsequently, 2 μL of LPS (1 mg/mL stock) was added to each well depending on the experimental group, plates were gently swirled, and incubation continued for 22 h. Post-incubation, culture supernatants were collected, centrifuged at 1,000× *g* for 20 min at 4°C, and the clarified supernatants were harvested for subsequent quantification of TNF-α levels using enzyme-linked immunosorbent assay (ELISA) according to the manufacturer's instructions.

2.7. Lymphocyte extraction

Mice were euthanized by cervical dislocation, sterilized in 75% ethanol for ~2 min, and dissected to isolate the spleen. The spleen was rinsed in ice-cold PBS and mechanically dissociated in a petri dish containing 1 mL of medium until only fibrous tissue remained. The homogenate was filtered through a 40-μm nylon mesh into a 50-mL conical tube. The dish and mesh were rinsed with additional medium (2-3 washes), with filtrates pooled. The cell suspension was transferred to a 15-mL conical tube and centrifuged at 1,000 × *g* for 10 min at RT. After supernatant removal, the pellet was resuspended in 2 mL of medium and adjusted to 0.25–0.5 × 10^8 cells/mL. For density gradient separation, 3 mL of Ficoll-Paque Plus was layered under 2 mL of cell suspension in a 15-mL tube, followed by centrifugation at 400× *g* for 30 min (RT). The lymphocyte-rich interface layer was carefully collected and transferred to a new 15-mL tube containing 6 mL of medium. After centrifugation (1000× *g*, 10 min, RT), the pelleted lymphocytes were washed once by resuspension in 3 mL of medium and recentrifuged. Finally, cells were resuspended in 1 mL of medium to generate splenic lymphocyte suspensions, with 50 μL aliquoted for cell counting.

2.8. Flow cytometry

Isolated splenic lymphocytes were resuspended in PBS and stained with Fixable Viability Stain 780 under light-protected conditions for 10-15 min. Cells were washed and centrifuged (350× *g*, 5 min) and then blocked with mouse BD Fc Block™ at 4°C for 5 min. Subsequently, cells were stained with fluorochrome-conjugated anti-CD3, anti-CD4, and anti-CD25 antibodies (optimally titrated) for 30 min at 4°C in darkness. Following another wash cycle, cells were resuspended in 200 μL of stain buffer and fixed with 200 μL of Fixation Buffer for 45 min at RT protected from light. After permeabilization using 1 mL of 1× Permeabilization Working Solution and centrifugation (600× *g*, 5 min, RT), intracellular staining was performed with anti-interferon (IFN)-γ, anti-interleukin (IL)-4, anti-IL-17A, and Treg markers separately per staining panel during incubation for 30 min (RT, dark). Cells were washed with 1.5 mL of stain buffer, centrifuged (600× *g*, 5 min, RT), and finally resuspended in 500 μL of stain buffer. The suspension was filtered through a 300-mesh sieve before acquisition on a flow cytometer pre-calibrated with compensation microspheres.

2.9. Detection of colonic cytokines

Colon tissue segments were excised, thoroughly rinsed in ice-cold PBS, and blotted dry on filter paper. After weighing (typically 30-40 mg per sample), tissues were transferred to microcentrifuge tubes. Samples were homogenized by adding 360 μL of PBS per 40 mg tissue weight along with a grinding bead, followed by mechanical disruption in a high-throughput tissue homogenizer (60 Hz, 150-180 seconds). The resulting homogenates were centrifuged at 12,000× *g* for 15 min at 4°C. Supernatants were collected and stored at -20°C until subsequent quantification of TNF-α, IL-17A, and IFN-γ levels using ELISA according to the manufacturer's protocols.

2.10. Statistical analyses

Data are expressed as the mean ± standard error of the mean (Mean ± SEM). Graphical representations were generated using GraphPad Prism 8.0. Histopathological images were acquired *via* whole-slide scanning, processed with the software SlideViewer, and exported as representative micrographs. Flow cytometry data were acquired and analyzed using the software CytExpert 2.5. Statistical analyses were performed in SPSS (IBM) using either one-way ANOVA or a Student's *t*-test as appropriate, with significance denoted as $*p < 0.05$, $**p < 0.01$, and $***p < 0.001$.

3. Results

3.1. *Trpa1* gene knockout does not alter the macroscopic structure or morphology of the mouse colon

To determine whether *Trpa1* knockout causes physiological structural changes in the mouse colon, the colon of euthanized *Trpa1*$^{-/-}$ and WT mice was dissected for comparative analysis. There were no significant

differences in colon length between WT mice (7.66 ± 0.19 cm) and *Trpa1*$^{-/-}$ mice (7.50 ± 0.24 cm) (Figure 1A). Colonic tissue segments from both groups were further fixed in 4% paraformaldehyde and paraffin sections were prepared. H&E, Alcian blue, and PAS staining were performed to compare colonic architecture and the number of goblet cells. As shown in Figure 1B, there were no discernible structural differences between the two groups. Crypts were tightly arranged in both, with no evidence of mucous layer disruption or inflammatory cell infiltration. Alcian blue and PAS staining further revealed no significant differences in the number of goblet cells in the colon of *Trpa1*$^{-/-}$ and WT mice (Figure 1C). Collectively, these findings indicate that *Trpa1* gene knockout does not induce alterations in the macroscopic structure or morphology of the mouse colon.

3.2. *Trpa1* knockout attenuates DSS-induced acute colitis in mice

The model of DSS-induced acute colitis in mice was used in this study to investigate the role of the TRPA1 channel in the pathogenesis of UC. Mice in the WT+DSS and *Trpa1*$^{-/-}$+DSS groups received 2.5% DSS in drinking water *ad libitum* for 7 days, while the NC group received sterile water throughout the modeling period.

Mice in both DSS-treated groups developed soft stools between days 2-4, with diarrhea appearing by day 5. By day 6, severe hematochezia and significant weight loss were prominent in most WT+DSS mice, whereas these symptoms were markedly milder in the *Trpa1*$^{-/-}$+DSS group. Both DSS-treated groups exhibited significant weight loss starting on day 6, with a significant difference in body weight between the WT+DSS and *Trpa1*$^{-/-}$+DSS groups emerging by day 7 (Figure 2A). The average daily DSS intake did not differ significantly between the two DSS-treated groups (Figure 2B), although the *Trpa1*$^{-/-}$+DSS group tended to have higher DSS intake compared to the WT+DSS group. The DAI increased abruptly from day 5 onwards in all DSS-treated groups. On day 7, the DAI was significantly higher in WT+DSS mice compared to that in *Trpa1*$^{-/-}$+DSS mice (Figure 2C). Spleen index analysis revealed significant differences between both DSS-treated groups and the NC group. While the *Trpa1*$^{-/-}$+DSS group tended to have a lower spleen index compared to the WT+DSS group, this difference was not significant. Upon necropsy, no enlargement of mesenteric lymph nodes was observed in DSS-treated groups compared to the NC group, suggesting that the colonic inflammation is mainly mediated by the innate immune response (Figure 2D). DSS-induced colitis resulted in significant colon shortening. Notably, *Trpa1*$^{-/-}$+DSS mice had a significantly greater colon length compared to that in WT+DSS mice (Figure 2E).

Histopathological examination of colon tissue *via* H&E staining revealed substantial structural damage in mice with DSS-induced UC, characterized by epithelial loss, crypt distortion with irregular architecture, and inflammatory cell infiltration into the submucosa.

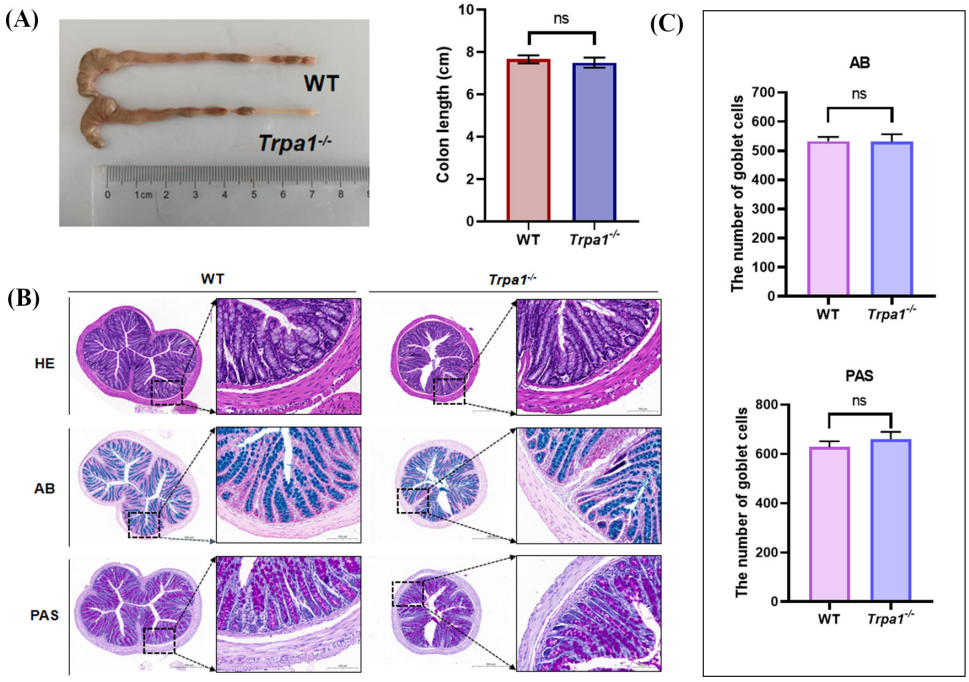

Figure 1. Comparison of colon morphology between *Trpa1*$^{-/-}$ and WT mice. (**A**) Representative images and statistical comparison of colon length between WT and *Trpa1*-knockout mice. (**B**) Representative cross-sectional images of colon tissue from WT and *Trpa1*-knockout mice stained with H&E, Alcian blue, and PAS; from left to right, magnifications are 100× and 400×. (**C**) Goblet cell counts corresponding to Alcian blue and PAS staining for each group in panel B.

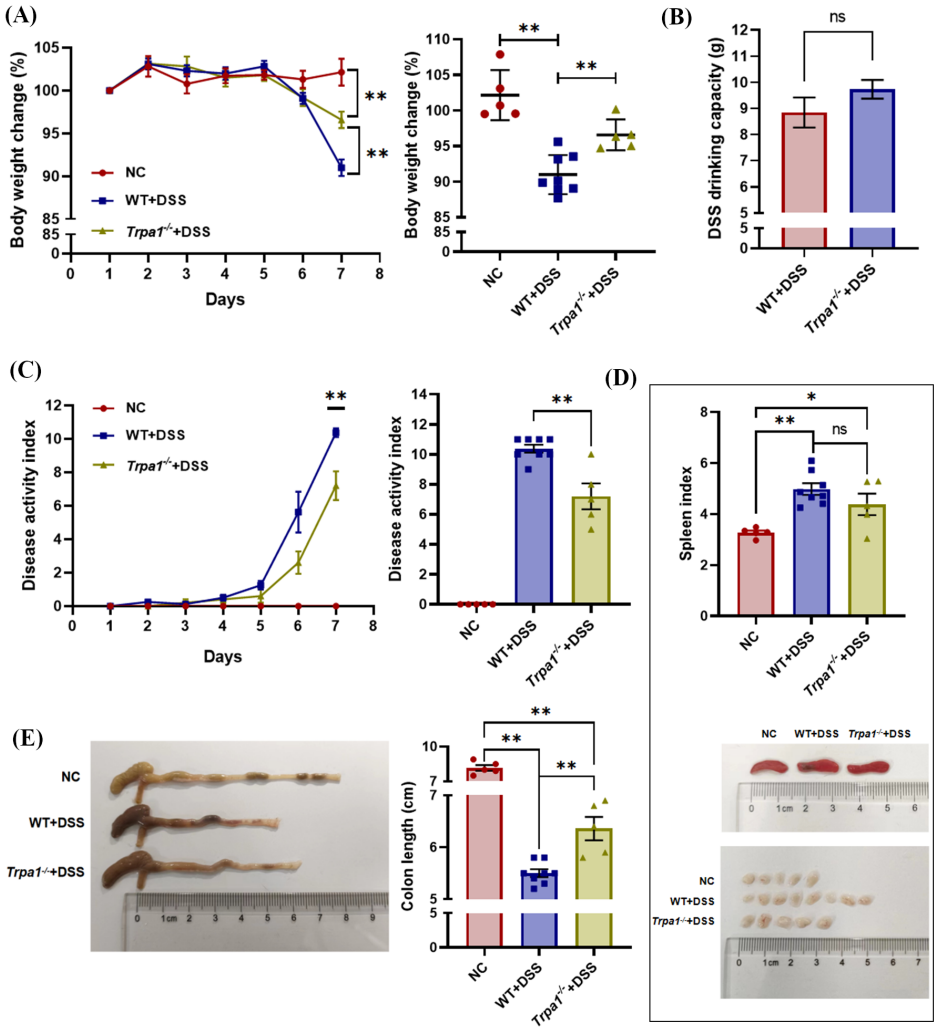

Figure 2. *Trpa1* knockout alleviates DSS-induced acute colitis in mice. (**A**) Time course of body weight loss (%) and comparison of body weight loss (%) on the final day among groups. (**B**) Average daily DSS consumption per mouse during modeling in WT+DSS and *Trpa1*$^{-/-}$+DSS groups. (**C**) DAI over the modeling period and DAI comparison among groups on the final day. (**D**) Spleen index (spleen weight [mg] / body weight [g]) and macroscopic comparison of spleen and mesenteric lymph nodes among groups. (**E**) Representative images and quantification of colon length among groups. *$p < 0.05$, **$p < 0.01$.

Compared to WT+DSS mice, the *Trpa1*$^{-/-}$+DSS group exhibited milder colon structural disruption and less epithelial loss. Consequently, the *Trpa1*$^{-/-}$+DSS group had significantly lower histopathological scores (Figure 3A). To further investigate the effect of *Trpa1* knockout on goblet cells in DSS-induced acute colitis, Alcian blue staining and PAS staining were performed to quantify goblet cells. Results indicated a significantly higher number of goblet cells in the colon of *Trpa1*$^{-/-}$ mice compared to that in the colon of WT mice, suggesting that *Trpa1* knockout may mitigate DSS-induced destruction of goblet cells (Figures 3B and 3C). Collectively, these findings indicate that genetic deletion of *Trpa1* significantly attenuates the symptoms of DSS-induced acute colitis in mice.

3.3. TRPA1 inhibitor attenuates DSS-induced acute colitis in mice

To further delineate the role of TRPA1 channels in acute colitis pathogenesis, the TRPA1-specific inhibitor A967079 was administered in a model of DSS-induced acute colitis, with 5-ASA serving as a positive control. Following 5 days of exposure to DSS, mice in the DSS+vehicle, DSS+A967079, and DSS+5-ASA groups all exhibited varying degrees of diarrhea and hematochezia. Compared to the DSS+vehicle group, mice treated with A967079 or 5-ASA had milder diarrhea and less pronounced weight loss (Figure 4A). By day 7, the DSS+A967079 group had a 8.4% reduction in weight loss relative to the DSS+vehicle group (11.1% *vs.* 19.5%, Figure 4B). Both the DSS+A967079 and DSS+5-ASA groups had significantly lower DAI scores than the DSS+vehicle group (Figures 4C and 4D). Post-mortem analysis revealed substantial attenuation of DSS-induced colon shortening in the DSS+A967079 and DSS+5-ASA groups compared to that in the DSS+vehicle group

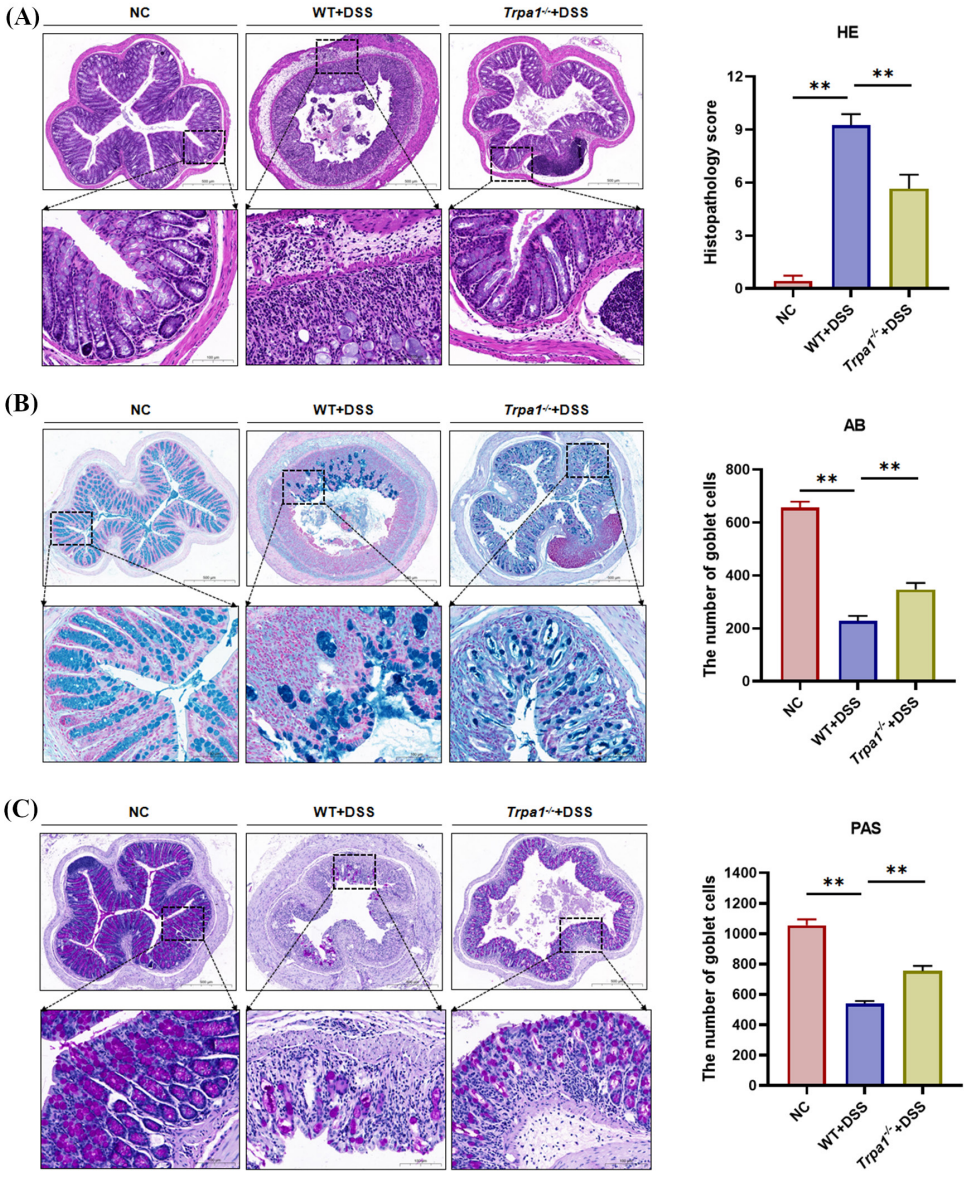

Figure 3. *Trpa1* knockout reduces colonic histopathological scores and goblet cells loss in mice with DSS-induced acute colitis. (**A**) Cross-sectional H&E staining of colon from DSS-induced acute colitis mice, with images shown at 100× (top) and 400× (bottom) magnification, followed by colonic histopathological scoring. Representative Alcian blue–stained (**B**) and PAS-stained (**C**) cross-sections of colon from DSS-induced acute colitis mice (top: 100×, bottom: 400× magnification) and quantification of goblet cells. $^{**}p < 0.01$.

(Figures 4E and 4F). Histopathological examination *via* H&E staining further confirmed reduced colonic damage in mice treated with the inhibitor (Figures 4G and 4H). Collectively, these results indicate that pharmacological inhibition of TRPA1 significantly ameliorates DSS-induced acute colitis in mice.

3.4. Inhibition of TRPA1 downregulates TNF-α secretion in RAW264.7 cells

Macrophages play a critical role in innate immune responses. As TRPA1 is expressed in macrophages (*19*), an LPS-induced RAW264.7 cell inflammation model was used to assess the impact of a TRPA1 inhibitor on cytokine secretion. To determine an appropriate drug concentration, RAW264.7 cells were co-incubated with varying concentrations of A967079 for 24 h. Cell proliferation was then assessed using a CCK-8 assay. As shown in Figure 5A, 30 μM A967079 had a mild inhibitory effect on RAW264.7 cell proliferation. Based on these results, A967079 concentrations of 1 μM, 3 μM, and 10 μM, which had no significant impact on cell proliferation, were selected for subsequent experiments. ELISA indicated that intervention with the TRPA1 inhibitor A967079 significantly reduced TNF-α secretion by RAW264.7 cells in a concentration-dependent manner (Figure 5B). This indicates that the TRPA1 inhibitor may have anti-inflammatory effects by suppressing the secretion of the macrophage-derived inflammatory cytokine TNF-α.

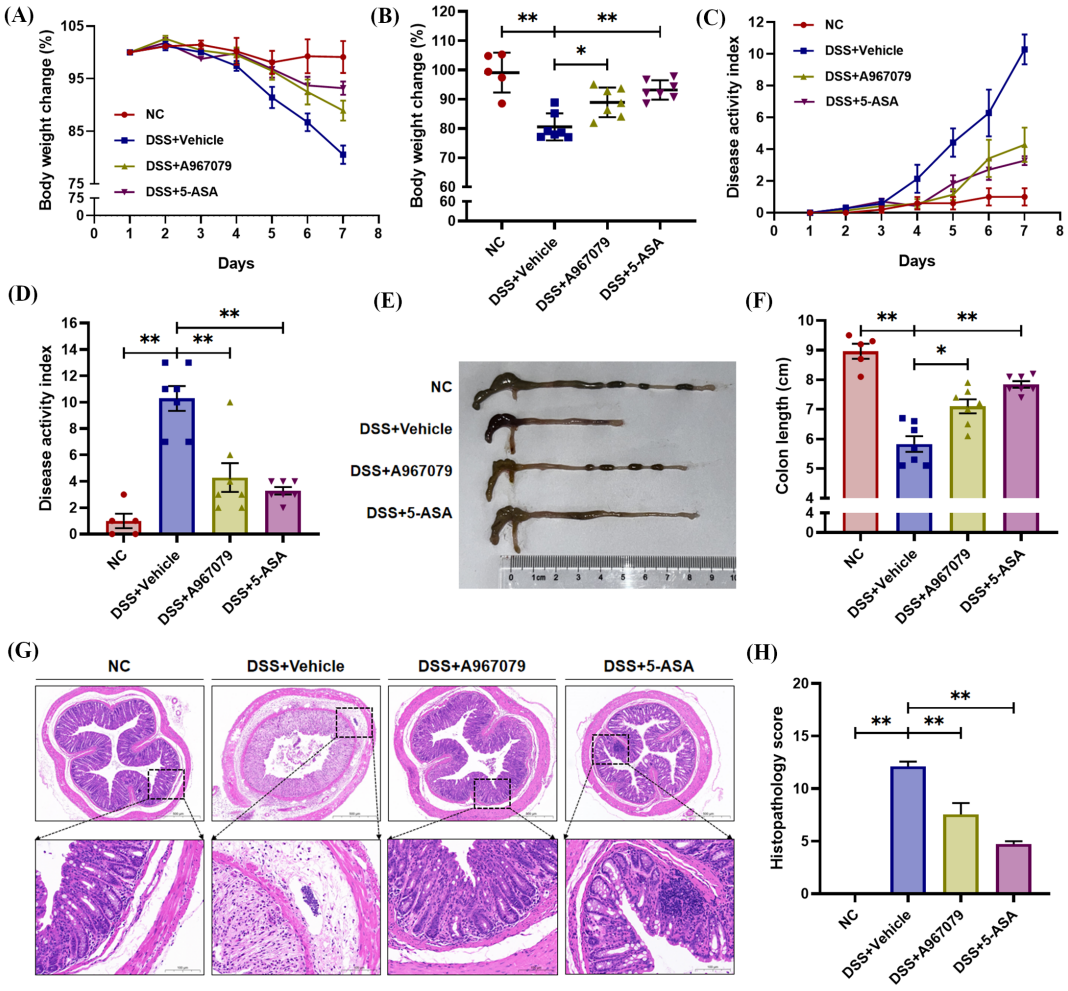

Figure 4. TRPA1 inhibitor alleviates DSS-induced acute colitis in mice. (A) Time course of body weight loss (%) in each group. (**B**) Comparison of body weight loss (%) among groups on the final day of modeling. (**C**) DAI over the modeling period in each group. (**D**) Comparison of DAI among groups on the final day. (**E**) Representative images of colon length from each group. (**F**) Quantitative analysis of colon length among groups. (**G**) Cross-sectional H&E staining of the colon in each group; images are shown at 100× (top) and 400× (bottom) magnification. (**H**) Colonic tissues from each group were scored according to the histopathological scoring criteria after H&E staining, and the results were statistically analyzed. $*p < 0.05$, $**p < 0.01$.

3.5. *Trpa1* knockout exacerbates DSS-induced subacute colitis in mice

UC is a chronic inflammatory disease that often presents with sudden and severe symptoms during acute flare-ups. To better model the characteristics of human UC, the authors previously established a DSS-induced murine model of subacute colitis (*20*). This model features prolonged colonic inflammation involving adaptive immunity, closely resembling the pathological features of UC. In this model, mice in both WT+DSS and *Trpa1*$^{-/-}$+DSS groups received 1% DSS in drinking water *ad libitum* for 30 days, followed by 1.5% DSS until modeling ended. Both DSS-treated groups developed diarrhea starting around day 15. Body weight in *Trpa1*$^{-/-}$+DSS mice began to decline significantly around day 33, whereas WT+DSS mice exhibited weight fluctuations without significant loss of weight (Figure 6A). DSS consumption did not differ significantly between the two groups throughout the experiment (Figure 6B). Compared to WT+DSS mice, *Trpa1*$^{-/-}$+DSS mice had significantly greater colon shortening, a higher DAI, and an increased spleen index, indicating a more severe inflammatory response (Figures 6C-6G).

Histopathological evaluation of colon tissue using H&E staining revealed severe colonic structural damage in mice with DSS-induced colitis, characterized by epithelial loss, crypt destruction with irregular arrangement, and lymphocyte infiltration into the submucosa (Figure 7A). Colonic damage was markedly more severe in *Trpa1*$^{-/-}$+DSS mice compared to that in WT+DSS mice, characterized by extensive epithelial loss and pronounced inflammatory cell infiltration. The knockout group had significantly higher histopathological scores. Alcian blue and PAS staining revealed a significantly greater reduction in the number of goblet cells in *Trpa1* knockout mice compared to that in WT mice (Figures 7B and 7C). Collectively, these findings

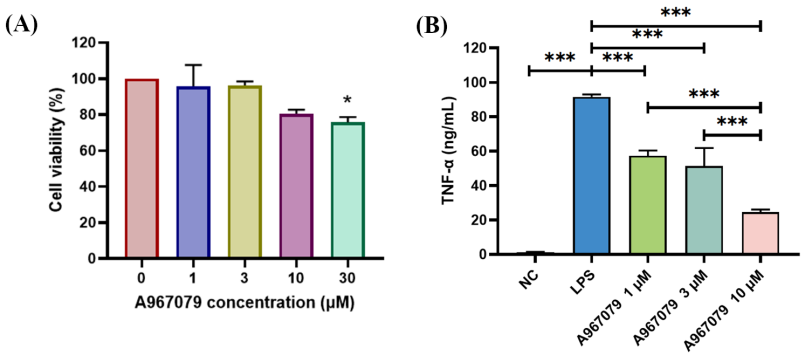

Figure 5. Inhibition of TRPA1 downregulates TNF-α secretion in RAW264.7 cells. (**A**) Effect of A967079 on RAW264.7 cell viability, assessed with a CCK-8 assay after 24 h of exposure to different concentrations of A967079. (**B**) Determination of the effect of a TRPA1 inhibitor on TNF-α secretion in LPS-stimulated RAW264.7 cells using ELISA. *$p < 0.05$, ***$p < 0.001$.

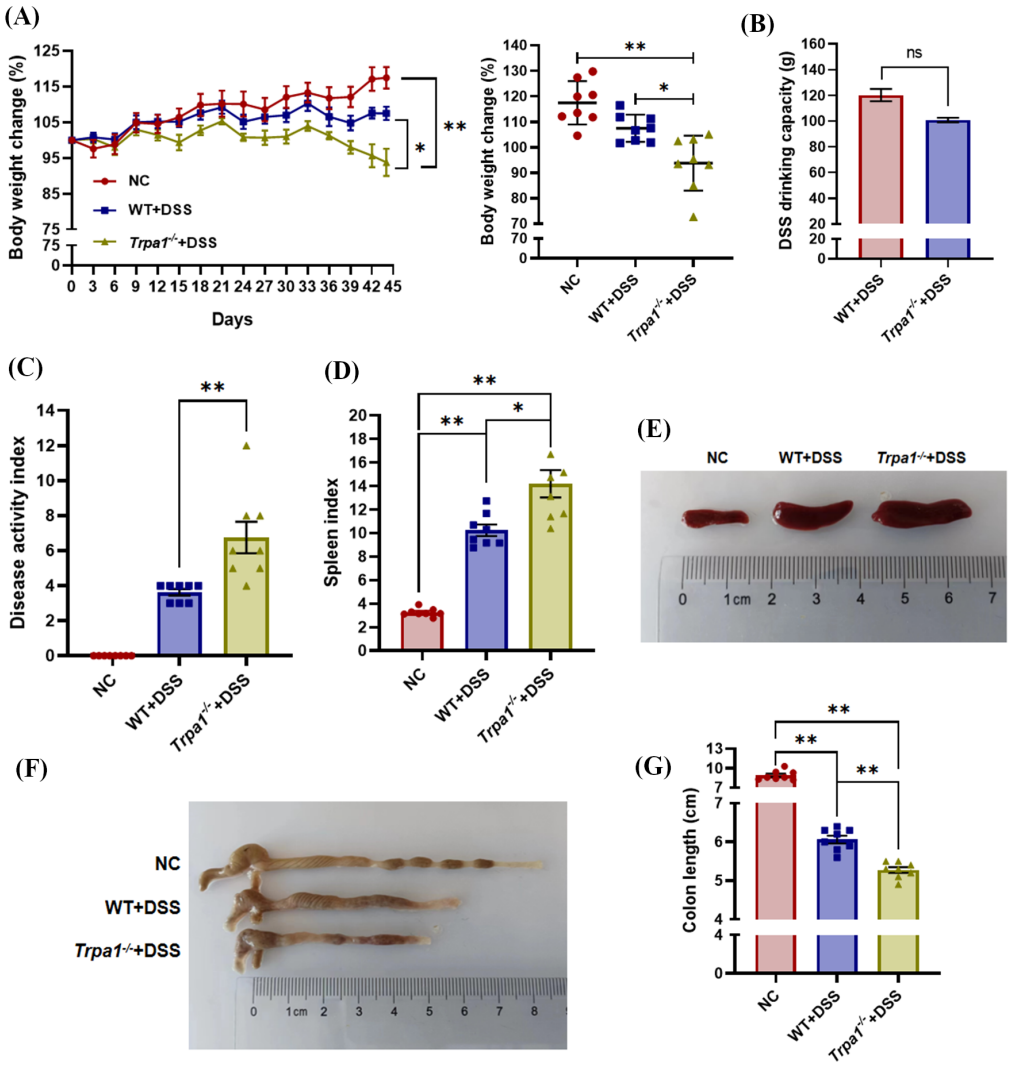

Figure 6. *Trpa1* knockout exacerbates DSS-induced subacute colitis in mice. (**A**) Time course of body weight loss (%) and comparison of body weight loss (%) among groups before tissue collection. (**B**) Water intake during modeling in the WT+DSS and *Trpa1*$^{-/-}$+DSS groups. (**C**) Comparison of DAI on the final day. (**D**) Comparison of the spleen index among groups (spleen index = spleen weight [mg] / body weight [g]). (**E**) Representative images of the spleen from each group. (**F**) Representative images of the colon from each group. (**G**) Quantitative analysis of colon length among groups. *$p < 0.05$, **$p < 0.01$.

indicate that *Trpa1* deletion has pro-inflammatory effects in subacute colitis in mice.

3.6. TRPA1 inhibitor exacerbates DSS-induced subacute colitis in mice

To further validate TRPA1's role in murine subacute colitis, mice were treated with the TRPA1 inhibitor A967079 (10 mg/kg, orally). Mice treated with A967079 exhibited exacerbated symptoms, including more severe weight loss, diarrhea with bloody stools, and colon shortening (Figures 8A-8E). Histopathological examination of colonic tissue using H&E staining was performed to assess pathological changes. As shown in Figure 8F, groups with DSS-induced subacute colitis displayed varying degrees of colonic mucosal damage, including disruption of the epithelium, destruction of crypts in the mucosal layer, and lymphocyte infiltration. Compared to the DSS+vehicle group, the DSS+A967079 group exhibited more severe colonic damage, aggravated inflammation, and had significantly higher histopathological scores (Figure 8G). Collectively, these results indicate that pharmacological inhibition of TRPA1 exacerbates DSS-induced subacute colitis in mice.

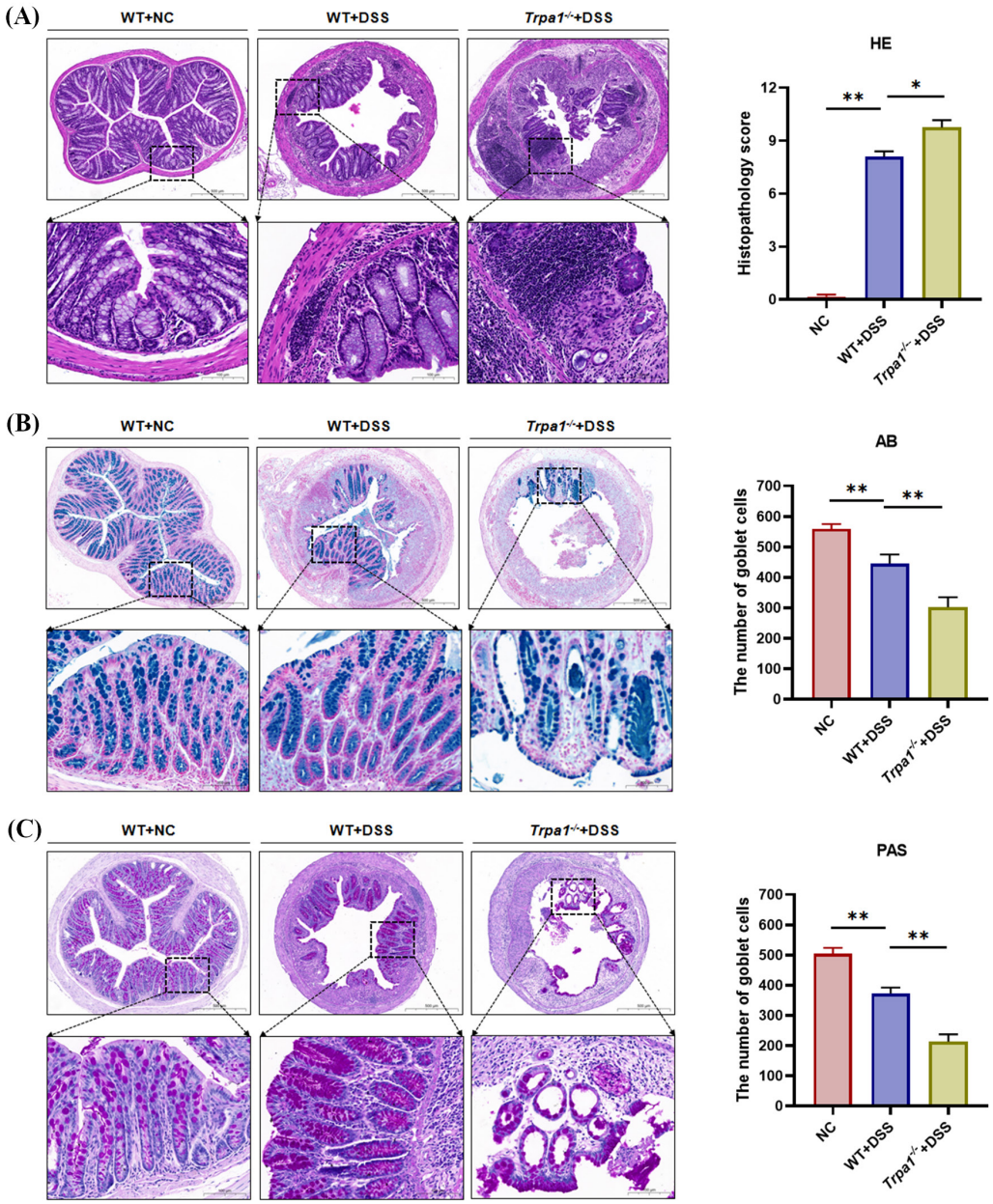

Figure 7. *Trpa1* knockout promotes inflammatory progression and goblet cell depletion in subacute colitis. (**A**) Cross-sectional H&E staining of the colon from mice with DSS-induced subacute colitis (from top to bottom, images are at 100× and 400× magnification) and histopathological scoring of colonic tissue. Representative images of cross-sectional Alcian blue (**B**) and PAS (**C**) staining of the colon from mice with DSS-induced subacute colitis (from top to bottom, images are at 100× and 400× magnification) and quantification of goblet cells. *$p < 0.05$, **$p < 0.01$.

3.7. *Trpa1* knockout promotes CD4+ T cell polarization towards the Th1 subtype

Our previous study indicated an elevated proportion of Th1 cells in a DSS-induced murine model of subacute colitis (*20*). Given that TRPA1 is expressed in CD4+ T cells (*19*), we hypothesized that TRPA1 might regulate CD4+ T cell polarization towards the Th1 subtype, thereby influencing DSS-induced subacute colitis. To verify this hypothesis, lymphocytes isolated from mice with colitis were analyzed using flow cytometry. Results indicated a significantly higher proportion of Th1 cells within the CD4+ T cell population in *Trpa1*$^{-/-}$+DSS mice (Figure 9A) compared to that in WT+DSS mice. There were no significant differences in the proportions of other CD4+ T cell subsets (Th2, Th17, and Treg).

To further confirm changes in CD4+ T cell subsets within the colonic tissue, colon segments from each group were homogenized, and cytokine levels (IFN-γ, IL-17A, TNF-α) were measured using ELISA. IFN-γ, a signature cytokine secreted by Th1 cells, and IL-17A, a specific cytokine produced by Th17 cells, play pivotal roles in the pathogenesis of colitis (*21*). TNF-α, a key inflammatory mediator, is secreted not only by macrophages but also by Th1 cells. ELISA revealed that colonic tissues from *Trpa1*$^{-/-}$+DSS mice contained significantly higher levels of IFN-γ compared to tissues from WT+DSS mice (Figure 9B), while TNF-α levels

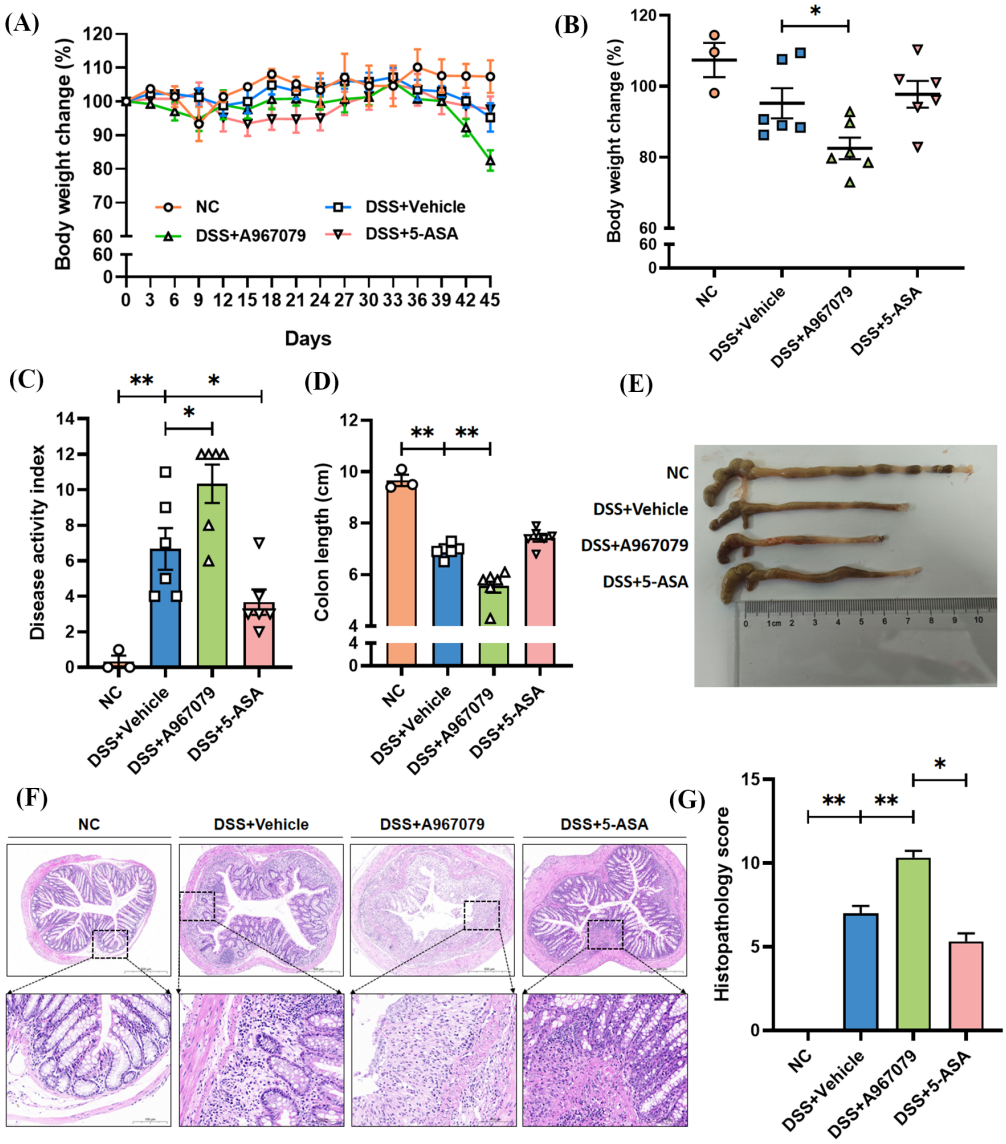

Figure 8. TRPA1 inhibitor exacerbates DSS-induced subacute colitis in mice. (**A**) Time course of body weight loss (%) in each group. (**B**) Comparison of body weight loss (%) among groups before tissue collection. (**C**) Comparison of DAI on the final day of the experiment. (**D**) Quantitative analysis of colon length among groups. (**E**) Representative images of colon length from each group. (**F**) Cross-sectional H&E staining of colon from each group; images are shown at 100× (top) and 400× (bottom) magnification. (**G**) Quantitative analysis of histopathological scores for colonic tissues from each group, assessed according to the histopathological scoring criteria after H&E staining. *$p < 0.05$, **$p < 0.01$.

tended to increase (Figure 9C). There were no significant differences in IL-17A levels between the two groups (Figure 9D). Collectively, these findings suggest that *Trpa1* deletion may facilitate CD4$^+$ T cell polarization towards the Th1 subtype, leading to increased secretion of pro-inflammatory cytokines and exacerbating colonic inflammation in a model of subacute colitis.

4. Discussion

The mouse model of DSS-induced acute colitis is currently the most commonly used animal model for UC. However, this model has several limitations, including a short modeling period, minimal involvement of the adaptive immune response, rapid progression of acute

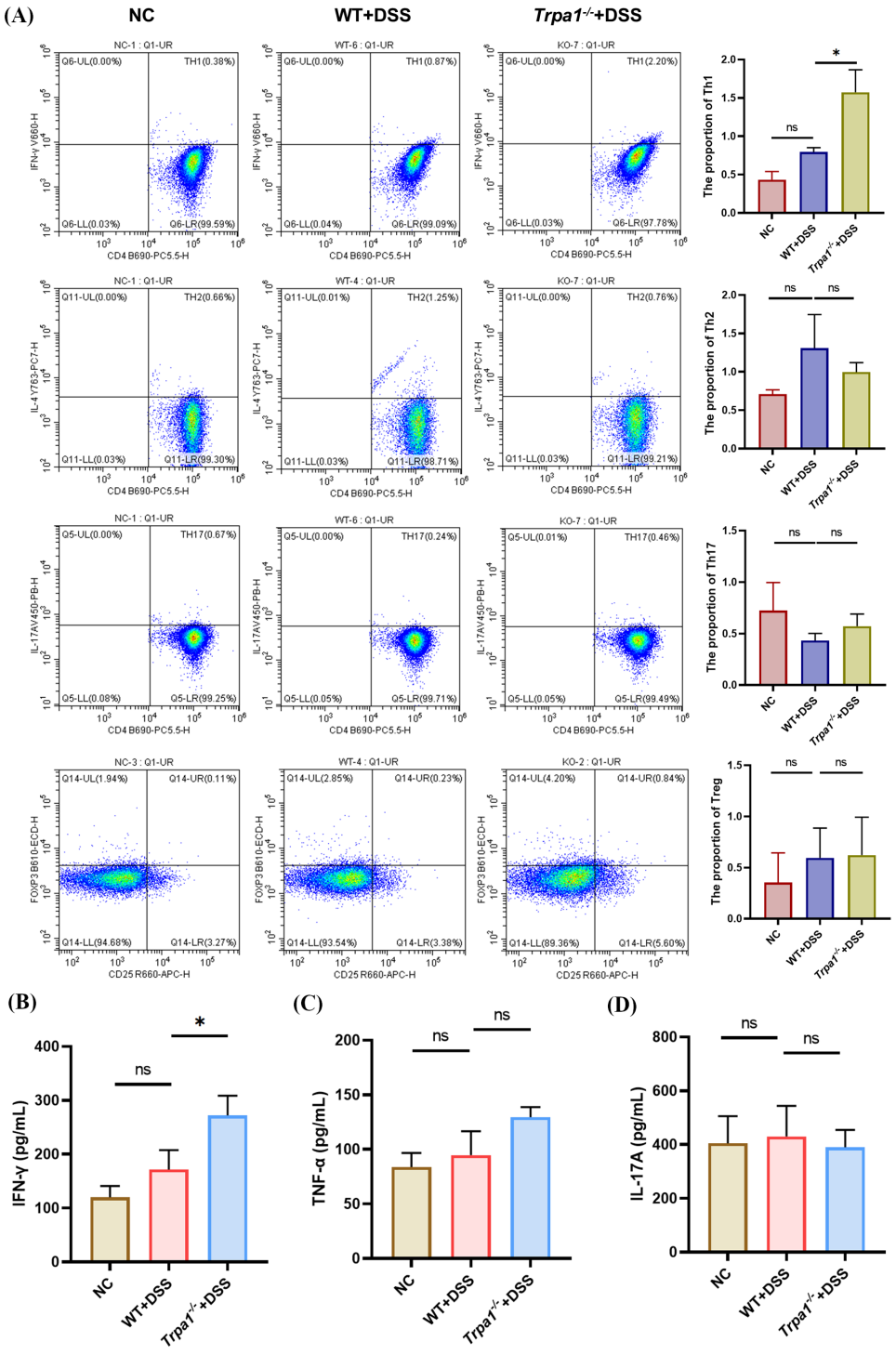

Figure 9. *Trpa1* knockout promotes CD4$^+$ T cell polarization towards the Th1 subtype. (**A**) Flow cytometry analysis of splenic lymphocytes after extraction. Mice were euthanized on day 45, and the spleen was removed to isolate lymphocytes for flow cytometry analysis. (**B-D**) Detection of IFN-γ, TNF-α, and IL-17A levels in colonic tissues using ELISA. *$p < 0.05$.

inflammation, and significant mouse mortality. To better recreate the pathological mechanisms of human UC, we created a novel murine model of DSS-induced subacute colitis in a previous study (*20*). This model features inflammation persisting for approximately 4 weeks, with a significantly increased proportion of adaptive immune cells, particularly Th1 cells, in the colonic mucosa, closely resembling the pathological characteristics of chronic inflammation.

The current study found that TRPA1 plays opposing roles in acute and subacute DSS-induced murine colitis. During the acute phase dominated by macrophages and neutrophils, TRPA1 inhibition attenuated colitis by suppressing the release of pro-inflammatory cytokines like TNF-α from macrophages. Conversely, during the subacute phase in which Th1-type $CD4^+$ T cells increased markedly alongside innate immune cells, TRPA1 inhibition exacerbated colonic inflammation, possibly by further increasing the proportion of Th1 cells. This aligns with the findings of Bertin *et al.*, which indicated that TRPA1 knockout worsened spontaneous colitis in IL-10-deficient mice and significantly upregulated Th1 proportions in lymphocytes (*19*). *In vitro*, TRPA1 knockout promoted the differentiation of naïve $CD4^+$ T cells into Th1 cells (*19*), which is consistent with our observations in a model of subacute colitis. The divergent functions of TRPA1 in different immune cell types likely underlie its dual role in colitis pathogenesis.

Results confirmed that TRPA1 inhibitors can ameliorate symptoms in an acute colitis model, which is consistent with prior studies. Engel *et al*. found that the TRPA1 inhibitor HC-030031 alleviated symptoms, reduced inflammatory markers, and improved histopathological damage in acute colitis (*18*). Our finding that TRPA1 inhibition exacerbates subacute colitis raises potential concerns regarding TRPA1 inhibition as a therapeutic strategy for human UC. However, human UC is primarily mediated by Th2 and Th17 cells within the adaptive immune compartment, unlike the Th1-driven pathology in our murine model of subacute colitis (*22*). Given the mutually inhibitory relationship between Th1 and Th2 differentiation, does TRPA1 inhibition-mediated Th1 promotion imply a corresponding reduction in Th2 cells, potentially offering a therapeutic benefit? Preliminary evidence supports this hypothesis. Cannabidivarin is a safe, non-psychoactive phytocannabinoid that acts as a TRPA1 desensitizing agent (*23*), and cannabis use that specifically involves this compound has been reported to alleviate symptoms in patients with UC (*23*). Moreover, a clinical study found that curcumin, which desensitizes and inhibits the TRPA1 channel, significantly reduced relapse rates in UC patients (*24,25*). Whether targeting TRPA1 inhibition in human UC could therapeutically reduce macrophage activity and lower Th2 cell proportions requires further investigation.

In summary, *Trpa1* gene knockout or pharmacological inhibition significantly ameliorates DSS-induced acute UC in a murine model but it exacerbates DSS-induced subacute UC. This dichotomy likely stems from the distinct functions of TRPA1 in macrophages versus $CD4^+$ T cells. Our findings provide new insights into the context-dependent roles of TRPA1 and suggest that TRPA1 may represent a context-specific and stage-dependent therapeutic target in UC.

Funding: None.

Conflict of Interest: The authors have no conflicts of interest to disclose.

References

1. Attauabi M, Madsen GR, Bendtsen F, Burisch J, Seidelin JB. The role of environmental factors prior to diagnosis on the activity and severity of inflammatory bowel diseases-Results from the prospective population-based Copenhagen Inflammatory Bowel Disease Inception Cohort. United European Gastroenterol J. 2025; 13:697-709.
2. Kobayashi T, Siegmund B, Le Berre C, Wei SC, Ferrante M, Shen B, Bernstein CN, Danese S, Peyrin-Biroulet L, Hibi T. Ulcerative colitis. Nat Rev Dis Primers. 2020; 6:74.
3. Ng SC, Shi HY, Hamidi N, Underwood FE, Tang W, Benchimol EI, Panaccione R, Ghosh S, Wu JCY, Chan FKL, Sung JJY, Kaplan GG. Worldwide incidence and prevalence of inflammatory bowel disease in the 21st century: A systematic review of population-based studies. Lancet. 2017; 390:2769-2778.
4. Bisgaard TH, Allin KH, Keefer L, Ananthakrishnan AN, Jess T. Depression and anxiety in inflammatory bowel disease: Epidemiology, mechanisms and treatment. Nat Rev Gastroenterol Hepatol. 2022; 19:717-726.
5. Sun Q, Jiang Z, Yang L, Liu H, Song P, Yuan L. Towards an Asian paradigm of inflammatory bowel disease management: A comparative review of China and Japan. Intractable Rare Dis Res. 2025; 14:192-202.
6. Mantzaris GJ. Thiopurines and methotrexate use in IBD patients in a biologic era. Curr Treat Options Gastroenterol. 2017; 15:84-104.
7. Kucharzik T, Koletzko S, Kannengiesser K, Dignass A. Ulcerative colitis-diagnostic and therapeutic algorithms. Dtsch Arztebl Int. 2020; 117:564-574.
8. Wehkamp J, Stange EF. Recent advances and emerging therapies in the non-surgical management of ulcerative colitis. F1000Res. 2018; 7:F1000.
9. Singh S, George J, Boland BS, Vande Casteele N, Sandborn WJ. Primary non-response to tumor necrosis factor antagonists is associated with inferior response to second-line biologics in patients with inflammatory bowel diseases: A systematic review and meta-analysis. J Crohns Colitis. 2018; 12:635-643.
10. Zhang M, Ma Y, Ye X, Zhang N, Pan L, Wang B. TRP (transient receptor potential) ion channel family: Structures, biological functions and therapeutic interventions for diseases. Signal Transduct Target Ther. 2023; 8:261.
11. Naert R, López-Requena A, Talavera K. TRPA1 Expression and pathophysiology in immune cells. Int J Mol Sci. 2021; 22:11460.

12. Lapointe TK, Altier C. The role of TRPA1 in visceral inflammation and pain. Channels (Austin). 2011; 5:525-529.
13. Nilius B, Owsianik G. The transient receptor potential family of ion channels. Genome Biol. 2011; 12:218.
14. Cheah EY, Burcham PC, Mann TS, Henry PJ. Acrolein relaxes mouse isolated tracheal smooth muscle *via* a TRPA1-dependent mechanism. Biochem Pharmacol. 2014; 89:148-156.
15. Bautista DM, Pellegrino M, Tsunozaki M. TRPA1: A gatekeeper for inflammation. Annu Rev Physiol. 2013; 75:181-200.
16. Russell FA, King R, Smillie SJ, Kodji X, Brain SD. Calcitonin gene-related peptide: Physiology and pathophysiology. Physiol Rev. 2014; 94:1099-1142.
17. Iannone LF, Nassini R, Patacchini R, Geppetti P, De Logu F. Neuronal and non-neuronal TRPA1 as therapeutic targets for pain and headache relief. Temperature (Austin). 2023; 10:50-66.
18. Engel MA, Leffler A, Niedermirtl F, *et al.* TRPA1 and substance P mediate colitis in mice. Gastroenterology. 2011; 141:1346-1358.
19. Bertin S, Aoki-Nonaka Y, Lee J, *et al*. The TRPA1 ion channel is expressed in $CD4^+$ T cells and restrains T-cell-mediated colitis through inhibition of TRPV1. Gut. 2017; 66:1584-1596.
20. Li J, Dou F, Hu S, Gao J. Involvement of adaptive immune responses in a model of subacute colitis induced with dextran sulfate sodium in C57BL/6 mice. Drug Discov Ther. 2023; 17:294-298.
21. Harbour SN, Maynard CL, Zindl CL, Schoeb TR, Weaver CT. Th17 cells give rise to Th1 cells that are required for the pathogenesis of colitis. Proc Natl Acad Sci U S A. 2015; 112:7061-7066.
22. Kałużna A, Olczyk P, Komosińska-Vassev K. The role of innate and adaptive immune cells in the pathogenesis and development of the inflammatory response in ulcerative colitis. J Clin Med. 2022; 11:400.
23. Pagano E, Romano B, Iannotti FA, *et al*. The non-euphoric phytocannabinoid cannabidivarin counteracts intestinal inflammation in mice and cytokine expression in biopsies from UC pediatric patients. Pharmacol Res. 2019; 149:104464.
24. Hanai H, Iida T, Takeuchi K, *et al*. Curcumin maintenance therapy for ulcerative colitis: Randomized, multicenter, double-blind, placebo-controlled trial. Clin Gastroenterol Hepatol. 2006; 4:1502-1506.
25. Csekő K, Beckers B, Keszthelyi D, Helyes Z. Role of TRPV1 and TRPA1 ion channels in inflammatory bowel diseases: Potential therapeutic targets? Pharmaceuticals (Basel). 2019; 12:48.

Received October 14, 2025; Revised January 10, 2026; Accepted January 15, 2026.

[§]These authors contributed equally to this work.

**Address correspondence to:*
Jianjun Gao, Department of Pharmacology, School of Pharmacy, Qingdao Medical College, Qingdao University, Qingdao, Shandong, China.
E-mail: gaojj@qdu.edu.cn

Shasha Hu, Department of Pathology, The Affiliated Hospital of Qingdao University, Qingdao, Shandong, China.
E-mail: huss0501@qdu.edu.cn

Released online in J-STAGE as advance publication January 23, 2026.